AIAA JOURNAL
Vol. 42, No. 2, February 2004

Revisiting a Wavy Bonded Single Lap Joint

Joseph D. Melograna* and Joachim L. Grenestedt†
Lehigh University, Bethlehem, Pennsylvania 18015

Single lap joints with wavy geometries have recently been proposed, and experiments have shown them to be superior in strength to conventional single lap joints for a particular carbon-fiber epoxy composite. The present study replicated one of the proposed wavy geometries, using a different carbon-fiber epoxy composite, a different adhesive, and a slightly different layup. The thickness and length of the current specimens were nearly identical to those of the previous study. Wavy and conventional specimens were manufactured, and tensile tests were performed. The wavy joints proved to be inferior to the conventional type. Numerical analyses were performed to explain the failure modes of the specimens. The reason for the poor performance of the present wavy joints is the high through-the-thickness stress, which initiated failure. The conventional specimens had lower through-the-thickness stress. The conventional specimens might exhibit higher stress concentrations near the ends of the adherends, but because of high toughness of the present composite this did not lead to failure. None of the specimen types failed by the adhesive.

I. Introduction

ADHESIVE single lap joints between composites have a large number of engineering applications. They are simple to manufacture, but suffer from load eccentricity, relatively high stress concentrations, and nonuniform shear stress along the bond line. In general, tensile peel stresses in the adhesive are more detrimental than shear stresses, and various ways to reduce the tensile peel stresses in particular have been devised (e.g., Refs. 1 and 2). Zeng and Sun[3] recently proposed a wavy single lap joint in which the two adherends are aligned, the stress concentrations at the ends of the adherends are reduced, the shear stress in the adhesive is more uniform, and the adhesive peel stress is reduced or even changed to compression. (In conventional single lap joints the two adherends are not aligned, and a load eccentricity and an associated bending moment thus result. In the wavy joint proposed by Zeng and Sun, the two adherends are aligned. However, because of lack of geometric symmetry, this wavy joint still possesses coupling between in-plane force and bending moment.) Experiments performed by Zeng and Sun using AS4/3501-6 carbon/epoxy adherends with $(90,0,90,0)_{2s}$ and $(0,90,0,90)_{2s}$ layups and FM73M film adhesive have shown that these wavy joints were considerably stronger than conventional single lap joints made with the same materials. In this paper the wavy joints of Zeng and Sun are replicated but using different materials, a different layup, and a different adhesive.

II. Specimen Manufacturing

Wavy and conventional single lap joints were manufactured and mechanically tested. The conventional specimens were molded on a flat piece of aluminum. For the wavy joints a computer-aided design (CAD) model with the geometry described by Zeng and Sun[3] was made, tool paths were generated, and an open aluminum mold was computer numerically controlled (CNC) machined to relatively close tolerances. The mold was made for the side of the adherends that would later be bonded, thus providing a well-defined bond line geometry.

Carbon-fiber specimens were made by using unidirectional T700/SE84HT carbon-fiber/epoxy prepreg from SP Systems. This is a fairly low-temperature cure system, processable with vacuum-only consolidation. The surface weight of the carbon fiber was 300 g/m^2, and the nominal matrix volume fraction of the prepreg was 37%. Specimens were made by laying up the prepregs on the aluminum mold, which had been coated with three layers of Frekote NC770 release agent. The layup was $(0,90,0)_s$, which differs from the $(0,90,0,90)_{2s}$ and $(90,0,90,0)_{2s}$ layups employed by Zeng and Sun. The prepregs were covered with one layer of DF62P9 porous release film, one layer of DB150 breather/bleeder, and vacuum bagged at 97% vacuum for an hour at 120°C. No external pressure, apart from the atmospheric, was applied. The heating and cooling gradients were always kept below 5°C/min. The total time in the oven was approximately 2.75 h. The thickness of the resulting specimens was approximately 1.95 mm, which is close to the 2.0 mm of the Zeng and Sun specimens.

The specimens were cut using a diamond cutoff wheel in a table saw. The surfaces that would be adhesively bonded were then acetone cleaned, lightly sanded using a 50-grit sandpaper, once again acetone cleaned, and bonded. The Hysol 9430 epoxy adhesive was used, and curing took place at room temperature (22°C). Small C clamps were used to fix the adherends and to provide clamping pressure. The resulting bondline was very thin, on the order of 0.1 mm or less. No means for exact control of the bondline thickness was employed. As will be seen later, this was not a problem because the specimens never failed by the adhesive. The adhesive was cured for at least 12 h at room temperature and postcured at 80°C for 1 h, before any mechanical testing was performed. For comparative reasons one specimen's adhesive was not postcured.

A majority of the specimens did not use tabs, and the experimental testing confirmed that tabs were not necessary because failure always occurred in the center of the specimens. A few specimens were manufactured with tabs and tested to failure. These "tabbed" joints did not show any appreciable differences in strength.

III. Mechanical Testing of the Joints

A Measurement Technology, Inc. (MTI)-modified 10-kip Instron universal test machine was used for the mechanical testing of the joints. All tests were performed under displacement control. The crosshead rate of motion was 0.508 mm/min (0.02 in/min). The particulars of all tests are summarized in Table 1.

The failure of the wavy joints started with transverse failure within the composite, rather than in the adhesive (cohesive failure) or in the interface between the composite and the adhesive (adhesive failure). Figure 1 supplies a side view of the first phase of the failure sequence. Note that one of the composite adherends has delaminated, but the adhesive is still intact. Upon further cross-head displacements, the

Received 18 April 2002; revision received 25 June 2003; accepted for publication 26 June 2003.

*Graduate Student, Department of Mechanical Engineering and Mechanics; currently Engineer, Materials Sciences Corporation, 500 Office Center Drive, Suite 250, Ft. Washington, PA 19034.

†Associate Professor, Department of Mechanical Engineering and Mechanics, 19 Memorial Drive West; jog5@lehigh.edu.

Table 1 Average forces per unit width and standard deviations of various joints manufactured with T700/SE84HT carbon-fiber/epoxy prepreg and Hysol 9430 adhesive

No.	Joint type	Nominal overlap length l, mm	Avg. P_{cr}, kN	Avg. τ_{cr}, MPa	Avg. F_x^E, N/mm	Standard deviation of F_x^E, N/mm
4	Wavy	25.4	9.35	14.11	389.24	55.75
4	Conventional	12.7	9.41	30.14	388.07	29.25
9	Conventional	25.4	15.56	25.14	616.66	54.33
6	Conventional	38.1	15.30	16.59	615.06	135.38
5	Conventional with tabs	25.4	15.95	24.35	633.03	84.54

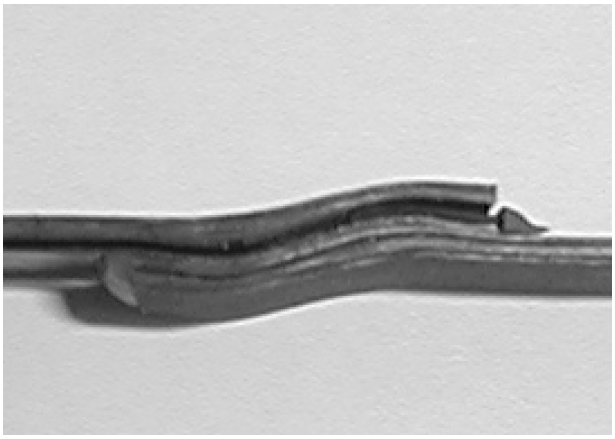

Fig. 1 Side view of wavy joint specimen after failure. The failure is within one of the composite adherends.

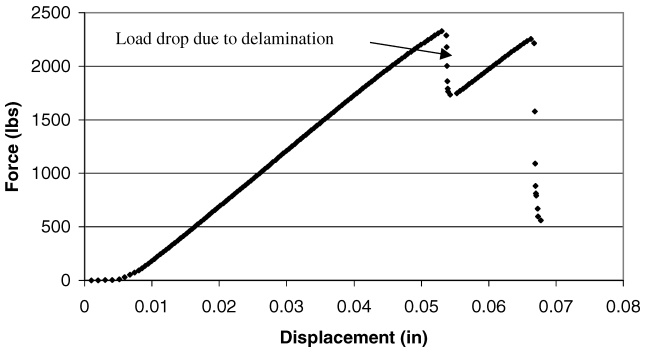

Fig. 2 Typical load-displacement curve for a wavy joint specimen. No slippage in the grips occurred, but the load dropped because of a delamination. After the initial delamination the load would drop, but it would rise during further cross-head displacements and the initial waviness would straighten out.

specimens would fail catastrophically by the adhesive. A typical load-displacement curve for the wavy joints is shown in Fig. 2, and it demonstrates the process. Observe that no slippage in the grips occurred, but the load dropped because of the delamination. After the initial delamination the load would drop, but it would rise during further crosshead displacements, and the initial waviness would straighten out. The load would continue to rise until the catastrophic failure. Only the single specimen that was not postcured failed within the adhesive (Fig. 3). The four specimens that were postcured failed at an average of 389 N per millimeter width of the specimen F_x^E. All specimens had a target width of 25.4 mm (1 in.) and a target overlap length of 25.4 mm (1 in.). The strengths of the joints were calculated as

$$\tau_{cr} = P_{cr}/wl \tag{1}$$

$$F_x^E = P_{cr}/w \tag{2}$$

where P_{cr} is the failure load, w is the width of the specimen, and l is the overlap length. F_x^E is the failure force per unit width of the specimen.

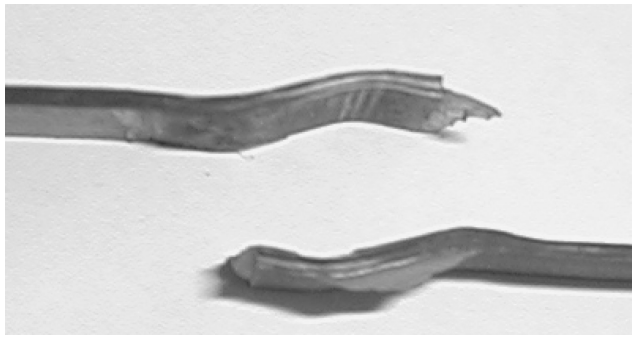

Fig. 3 Side view of tested specimen whose adhesive had not been postcured. No specimens with postcured adhesives failed in the adhesive.

Conventional joints with three different overlap lengths (12.7, 25.4, and 38.1 mm) were also manufactured, using the same materials and adhesive, and mechanically tested. Initially, tabs were not used on the conventional specimens either. Rather, a pair of self-aligning grips was used, and this minimized the effect of the fact that the two adherends were not aligned. Also in these conventional joints, failure occurred within the composite as opposed to in the adhesive. Delaminations starting from the ends of the adherends and propagating parallel to the joints, but not along the glue line, were quite evident in the 38.1-mm overlap specimens. An average force per unit width of the specimen of 388 N/mm was attained with the 12.7-mm overlap length. This value is comparable to the strength of the wavy joint with an overlap length of 25.4 mm. Conventional specimens with overlap lengths of 25.4 and 38.1 mm performed similarly with values of average force per unit width at approximately 615 N/mm. These results imply that these specimens had approached an asymptotic value of strength. The specimens with wavy joints were considerably weaker than the specimens with conventional single lap joints with the same overlap lengths.

For comparative reasons additional tests using end tabs on conventional single lap joints with overlap lengths of approximately 25.4 mm were performed. The reason behind the tabs was to further reduce possible misalignment problems and to facilitate gripping. The tabs were made of the same carbon-fiber composite and were bonded to the adherends with Hysol 9430 adhesive. The lengths of the tabs were approximately 38 mm. Five specimens were tested to failure. These particular joints had an average strength per unit width of approximately 630 N/mm. No further testing with tabs was carried out on conventional single lap joints of different overlap lengths because of the minimal difference in strength. The difference in strength between tabbed and untabbed specimens was approximately 2%.

The mechanical tests suggest that the joints failed by transverse tension or shear in the composite rather than at the adhesive/composite interface. For this end transverse tensile tests were performed as outlined in the end of the next section.

IV. Determination of Material Properties for the T700/SE84HT Carbon/Epoxy

Material properties were experimentally measured for the present material system as outlined next. The properties were needed for the subsequent numerical analyses.

Table 2 Results from a vibration test on a 90 × 116 mm rectangular plate with a 0_2 layup[a]

Mode	f_i^{exp}	f_i^{fem}	Difference, %	T700/SE84HT 0_2
1	120.062	118.144	1.60	——
2	166.624	163.917	1.62	——
3	324.912	325.946	0.32	$E_1 = 127.65$ GPa, $E_2 = 8.55$ GPa
4	361.496	354.101	2.05	$G_{12} = G_{13} = 9.82$ GPa
5	567.389	598.109	5.41	$G_{23} = 3.08$ GPa, $\nu_{12} = 0.294$
6	642.221	640.488	0.27	$\rho = 1377$ kg/m^3
7	751.974	775.447	3.12	——
8	876.028	842.005	3.88	——

[a]The material properties served as the design variables during the optimization process. The values listed led to numerical eigenfrequencies that were in close agreement with the experimental eigenfrequencies.

Table 3 Results from a vibration test on a 90 × 118 mm rectangular plate with a (0,90,0,90,0) layup[a]

Mode	f_i^{exp}	f_i^{fem}	Difference, %	T700/SE84HT (0,90,0,90,0)
1	427.937	414.927	3.04	——
2	608.935	577.042	5.24	——
3	999.318	1020.301	2.10	$E_1 = 128.08$ GPa, $E_2 = 10.99$ GPa
4	1598.733	1588.258	0.66	$G_{12} = G_{13} = 10.09$ GPa
5	1724.066	1729.599	0.32	$G_{23} = 3.86$ GPa, $\nu_{12} = 0.291$
6	1863.805	1917.185	2.86	$\rho = 1394$ kg/m^3
7	2089.631	2020.292	3.32	——
8	2386.197	2474.525	3.70	——

[a]The material properties served as the design variables during the optimization process. The values listed led to numerical eigenfrequencies that were in close agreement with the experimental eigenfrequencies.

Table 4 Results from a vibration test on a 90 × 120 mm rectangular plate with a 0_{16} layup[a]

Mode	f_i^{exp}	f_i^{fem}	Difference, %	T700/SE84HT 0_{16}
1	903.165	877.694	2.82	——
2	1433.606	1367.980	5.28	——
3	2403.626	2405.013	0.06	$E_1 = 124.68$ GPa, $E_2 = 7.99$ GPa
4	2972.711	2875.625	3.27	$G_{12} = G_{13} = 11.59$ GPa
5	4488.323	4669.841	4.04	$G_{23} = 3.60$ GPa, $\nu_{12} = 0.299$
6	4630.065	4720.686	1.96	$\rho = 1351$ kg/m^3
7	5942.120	6082.013	2.35	——
8	6634.970	6610.307	0.37	——

[a]The material properties served as the design variables during the optimization process. The values listed led to numerical eigenfrequencies that were in close agreement with the experimental eigenfrequencies.

A. Elastic Properties

The elastic properties of the TH700/SE84HT carbon/epoxy from SP Systems were measured using an in-house vibration test. In short, this technique relies on experimentally measured eigenfrequencies of a composite plate, and finite element analysis (FEA). An optimization method is used to minimize the differences in eigenfrequencies between the experiments and FEA, using the elastic stiffnesses as variables. In the present study three different carbon-fiber plates were investigated. These three plates had the following dimensions and layups: a 90 × 116 mm rectangular plate with a 0_2 layup, a 90 × 118 mm rectangular plate with a (0,90,0,90,0) layup, and a 90 × 120 mm rectangular plate with a 0_{16} layup. A summary of the experimental and numerical eigenfrequencies for these three plates along with the elastic properties associated with those eigenfrequencies is given in Tables 2–4. The elastic properties obtained for the three different plates are in close agreement with each other. Rounded averages of these material properties for T700/SE84HT are given in Table 5. Elastic and shear moduli are rounded to the nearest 0.5 GPa.

Table 5 Material properties for the T700/SE84HT obtained by rounding the averages of the results in Tables 2–4

Property	Value
E_1	127 GPa
E_2	9 GPa
G_{12}, G_{13}	10.5 GPa
G_{23}	3.5 GPa
ν_{12}	0.295
ρ	1375 kg/m^3

B. Longitudinal Tensile Strength

Unidirectional longitudinal tensile strength of the T700/SE84HT was determined in accordance with the ASTM D 3039 Standard Test Method for Tensile Properties of Polymer Matrix Composite Materials.[4] Specimens were cut from a carbon-fiber plate with a 0_3 stacking sequence. As recommended in the American Society for Testing and Materials (ASTM) standard, the thickness of the specimens was approximately 1 mm, the width was approximately 15 mm, and the overall length was approximately 250 mm. Tabs with a length of approximately 56 mm and a thickness of approximately 1.5 mm were used. The tab material was a vacuum-assisted resin transfer molded composite, made of a Hexcel 7725 glass fiber weave and SP Systems' Prime 20 epoxy. The glass fiber tabs were oriented at 45 deg to the loading direction to provide a soft interface. The tabs were adhesively bonded to the carbon fiber with Hysol 9430. Twelve specimens were tested. ASTM D 3039 suggests inserting the specimens so that the end of the grips goes beyond the

edge of the tabs by 10–15 mm and thus reducing the risk for delaminating the tabs from the specimens. The particular grips used during testing had the same length of 56 mm as the tabs. Therefore, selected specimens were cut in order to reduce tab length. Strengths obtained between the varying tab length specimens did not show appreciable differences. An average longitudinal tensile strength of 1.93 GPa with a standard deviation of 0.16 GPa was obtained.

C. Longitudinal Compressive Strength

Longitudinal compressive strength of the T700/SE84HT composite was measured using the ASTM D 6641-01 Standard Test Method for Determining the Compressive Properties of Polymer Matrix Composite Laminates Using a Combined Loading Compression Test Fixture.[4] All specimens had a target width of 25.4 mm and a target length of 140 mm. Specimens with more than 50% of 0-deg plies are considered nonstandard because of the high-fixture clamping forces needed to prevent end crushing. Excessive clamping forces could cause erroneously low strength results. In addition, when specimens with 0-deg outer plies are used, the local stress concentrations at the ends of the specimen gauge section can lead to premature failure and, consequently, low strength results. Specimens with the layups $(90,0)_{2s}$ and (0,90,0,90,0), the latter violating both the suggested maximum of 50% of 0-deg plies and the recommendation to avoid 0-deg plies on the surfaces, were manufactured for compression testing. A torque of 2.3–2.8 Nm (20–25 in.-lb) was applied to the clamping screws as recommended in the standard.

Compressive strength of a ply oriented in the 0-deg direction was calculated by using a backout factor as proposed by Welsh and Adams.[5] Back out factors for the $(90,0)_{2s}$ and (0,90,0,90,0) layups were 2.25 and 1.86, respectively. Observe that the uniaxial compression test leads to tensile stresses in the 90-deg plies (in the axial direction), thus resulting in backout factors larger than 2 and 1.67, respectively. Average longitudinal compressive strengths of a unidirectional 0-deg ply in the $(90,0)_{2s}$ and (0,90,0,90,0) layups were 1.09 GPa (0.07 GPa standard deviation) and 0.76 GPa (0.14 GPa standard deviation), respectively. As expected, the compressive strength of the 0-deg plies in the (0,90,0,90,0) specimens was appreciably lower than that of the $(90,0)_{2s}$ specimens. The results from the $(90,0)_{2s}$ specimens were used as the compressive strength for the present paper.

D. Interlaminar Shear Strength

Interlaminar shear strength of the T700/SE84HT composite was obtained using the ASTM D 2344-84 Standard Test Method for Apparent Interlaminar Shear Strength of Parallel Fiber Composites by Short-Beam Method.[4] Specimens were cut (with a diamond blade) from a composite plate with the stacking sequence 0_{16}. According to the standard, carbon-fiber specimens should have a length/thickness ratio of 6. Target lengths were 31.2 mm while the thickness of the specimens was approximately 5.2 mm. Widths of all specimens were approximately 5.75 mm. Eleven specimens were tested to failure. Apparent shear strength was calculated according to the standard, resulting in an average shear strength of 72.5 MPa with a standard deviation of 2.35 MPa.

E. Transverse Tensile Strength

Because the joint specimens failed in what appeared to be a transverse tensile mode, transverse tensile tests were performed. At large, the tests were performed according to the ASTM C 297-94 Standard Test Method for Flatwise Tensile Strength of Sandwich Constructions.[4] Although initially developed for sandwich constructions, this test method is commonly used for transverse tensile testing of fiber-reinforced composites.

Square chip-like specimens made from the flat carbon-fiber laminates were adhesively bonded to two steel blocks and subjected to transverse tensile loads. Figure 4 shows a specimen after testing. The layup was the same as for all joint specimens, that is, $(0,90,0)_s$. This layup was chosen for two reasons: the residual stresses should be similar to those in the joint specimens, plus the tests using this layup would reveal whether the interlaminar tensile strength between a 0 and 90 ply is lower than the intralaminar strength. The

Fig. 4 Transverse tensile test specimen after failure. The failure in this $(0,90,0)_s$ specimen is intralaminar.

tensile strength was calculated as $\sigma_{cr} = P_{cr}/(w_1 w_2)$, where P_{cr} is the failure load and w_1 and w_2 are the lengths of the sides of the specimen. Nominally, $w_1 = w_2 = 35$ mm. The failure load was measured using an MTI-modified 10-kip Instron universal test machine. Two sets of transverse tensile tests, using different loading rates [0.508 mm/min (0.02 in./min) and 0.0254 mm/min (0.001 in./min), respectively] were performed. The different loading rates were used to examine the rate sensitivity of the transverse tensile strength. ASTM C 297-94 suggests a rate of 0.508 mm/min (0.02 in./min) and that the maximum load should occur between 3 to 6 min. However, that standard was developed for sandwich specimens. The present specimens, when tested at the rate of 0.0254 mm/min (0.001 in./min), failed after approximately 40 min.

All specimens were bonded to steel blocks, using the Hysol 9430 epoxy adhesive. The steel blocks were bead blasted and acetone cleaned before bonding. Eight specimens were tested at the higher loading rate, and with one exception all specimens failed completely within the composite. The specimen that failed in the adhesive by the steel blocks was discarded. The average transverse tensile strength of the remaining seven specimens was 21.25 MPa with a standard deviation of 1.79 MPa. The specimens failed mainly by intralaminar fracture, that is, within a single ply. The particular layup for these specimens was chosen in order to elucidate whether the interlaminar strength of the 0/90 interface was lower than the intralaminar strength. This proved not to be the case because all failures were intralaminar. Similar failure modes were observed for the lower loading rate. The lower strain rate average transverse tensile strength was 17.61 MPa with a standard deviation of 1.39 MPa. The transverse strength was thus 15% lower for the lower strain rate than for the higher.

F. Interlaminar Fracture Toughness

The interlaminar fracture toughness of T700/SE84HT carbon-fiber composite was calculated using ASTM D 5528-94a Standard Test Method for Mode I Interlaminar Fracture Toughness of Unidirectional Fiber-Reinforced Polymer Matrix Composites[4] as a guide. Double-cantilever-beam (DCB) specimens were manufactured using a 0_{12} laminate of T700/SE84HT carbon-fiber/epoxy prepreg. Specimens were cut out of the panel with a waterjet cutter to approximate lengths of 127 mm (5 in.) and widths of 25.4 mm (1 in.). Wrightlon® 5200 High Performance Fluoropolymer Release Film-ETFE from Airtech International (nominal length of 62.5 mm) was inserted at the midplane of the laminate during the layup process. The nominal film thickness was 15 μm (0.0006 in.), which is slightly more than the 13 μm suggested in the standard. Grit-blasted piano hinges were bonded to both sides of the specimens using Hysol 9430 adhesive.

Four specimens were tested in a 1-kip Instron universal test machine at various crosshead displacement rates (1–5 mm/min). Crosshead displacement and load were recorded throughout the tests. After initial delamination growth each specimen underwent three to five unloading/reloading cycles (Fig. 5). Each unloading/reloading

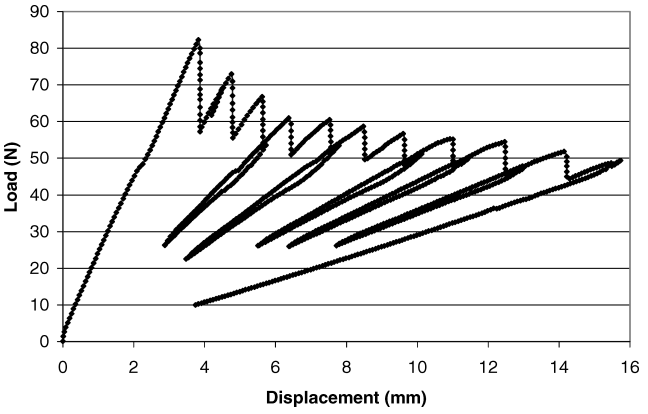

Fig. 5 Typical load vs displacement curve for a DCB specimen during mode I interlaminar fracture toughness testing.

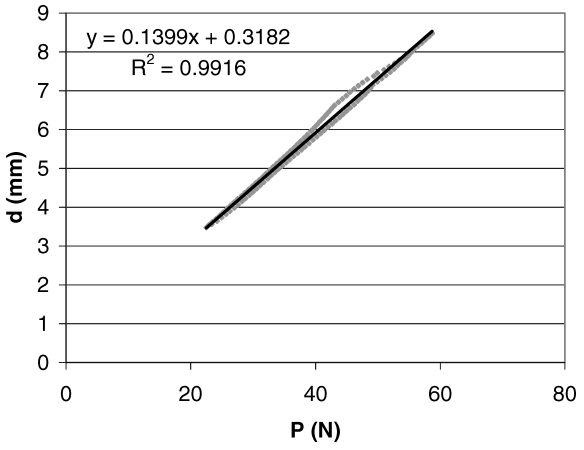

Fig. 6 Typical displacement vs load curve for a single unloading/reloading cycle of a DCB specimen. The compliance is determined from the slope of the linear regression.

cycle was analyzed to determine the compliance C, degree of plastic deformation, approximate crack length a, and energy release rate G_I. The compliance C was determined by fitting a straight line through the unloading/reloading data points plotted on a displacement vs load graph (Fig. 6). The degree of plastic deformation could be implied from the line's intercept. The crack length a was calculated from simple beam theory as follows:

$$a = \sqrt[3]{CEh^3B/8} \tag{3}$$

where C is the compliance, E is the tensile modulus of elasticity, h is the midplane thickness, and B is the width of the specimen. The energy release rate was then calculated by

$$G_I = \frac{P^2}{2B}\frac{\partial C}{\partial a} = \frac{12P^2a^2}{Eh^3B^2} \tag{4}$$

An average energy release rate of 479.5 J/m^2 with a standard deviation of 92.23 J/m^2 was calculated by averaging energy release rates from the individual unloading/reloading cycles from all four specimens. ASTM D 5528-94a reports an energy release rate of 85 J/m^2 for AS4/3501-6 carbon-fiber/epoxy.[4] The value obtained for T700/SE84HT is five to six times larger.

V. Numerical Analysis

The joint specimens manufactured were numerically analyzed using the ANSYS[6] commercial finite element code. Two-dimensional plane-strain deformation was assumed. The Hysol 9430 adhesive was assumed to have a thickness of 0.1 mm. Material nonlinearities for the T700/SE84HT carbon-fiber composite were ignored, and the unidirectional material was assumed to be transversely isotropic. The elastic properties were measured using a modal technique, as previously explained. Elastic constants and strengths used in numerical analyses for both the present study's and Zeng and Sun's materials are given in Tables 6–8.

Table 6 Elastic and strength properties of T700/SE84HT

Property	Value
E_1	127 GPa
E_2	9 GPa
E_3	9 GPa
F_{1t}	1930 MPa
F_{2t}	21.25 MPa
G_{12}	10.5 GPa
G_{13}	10.5 GPa
G_{23}	3.5 GPa
F_{1c}	1090 MPa
F_{2c}	——[a]
ν_{12}	0.295
ν_{13}	0.295
ν_{23}	0.286
F_6	72.5 MPa

[a]The transverse compression strength was not measured because it was not considered relevant for the present study.

Table 7 Elastic and strength properties of AS4/3501-6[3,7]

Property	Value
E_1	148 GPa
E_2	10.5 GPa
E_3	10.5 GPa
F_{1t}	2280 MPa
F_{2t}	57 MPa
G_{12}	5.61 GPa
G_{13}	5.61 GPa
G_{23}	3.17 GPa
F_{1c}	1440 MPa
F_{2c}	228 MPa
ν_{12}	0.3
ν_{13}	0.3
ν_{23}	0.59
F_6	71 MPa

Table 8 Material properties for Hysol 9430 adhesive and FM73M film adhesive

Property	FM73M	Hysol 9430 adhesive
E_g	2.2 GPa	2.621 GPa
ν_g	0.31	0.35
σ_{YS}	33 MPa	37 MPa

Plane-strain elements PLANE82 were used for both the adherend and the adhesive. Each ply of the composite was modeled with four elements through the thickness, whereas the adhesive was modeled with two elements through the thickness. In the overlap region there were 112 elements across for both the adherends and adhesive. Outside of the joint region there were 140 elements across with four elements through the thickness of each ply. The same scheme was employed for the present analyses of Zeng and Sun's joints, except that only two elements through the thickness of each composite ply were used. This was done because a ply of AS4/3501-6 had a thickness of 0.125 mm while a ply of T700/SE84HT had a thickness of 0.325 mm. Similar finite element (FE) models were created for conventional single lap joints of both materials.

For both the wavy and conventional single lap joints, the experimentally measured average forces per unit width F_x^E were applied to the specimens. The global x direction was oriented parallel to the axis of loading. Both adherend ends were clamped against displacements in the y direction and rotations. Two different kinds of

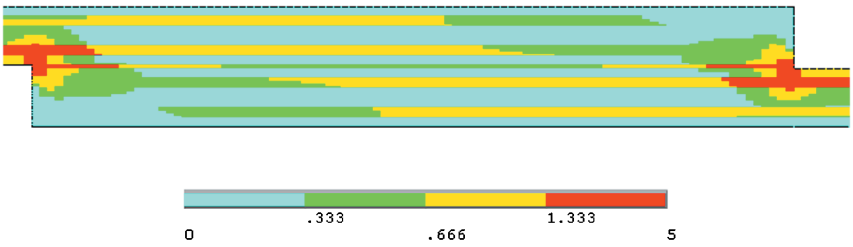

Fig. 7 Contour plot of the parameter MNS obtained from a geometrically nonlinear analysis of a conventional single lap joint with T700/SE84HT adherends and Hysol 9430 adhesive.

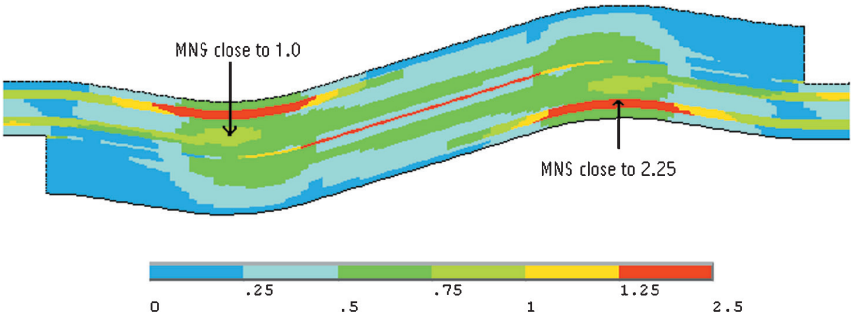

Fig. 8 Contour plot of the parameter MNS obtained from a geometrically nonlinear analysis of a wavy joint with T700/SE84HT adherends and Hysol 9430 adhesive. The left arrow points to a region where MNS = 1, which corresponds to the through-the-thickness stress. The right arrow points to a region where MNS = 2.25. This region corresponds to transverse in-plane stress. Very likely, transverse matrix cracks will form here.

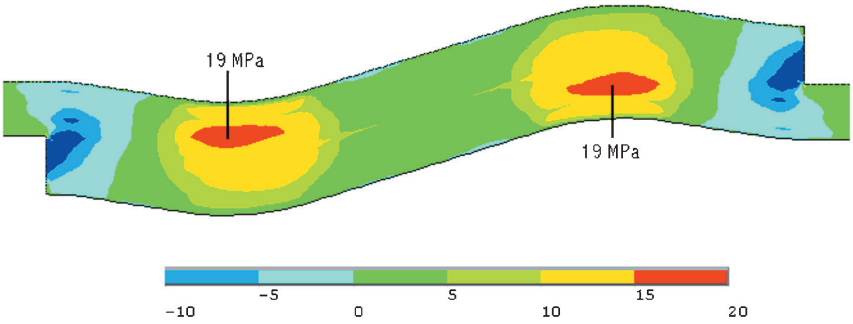

Fig. 9 Contour plot of the through-the-thickness stress obtained from a geometrically nonlinear analysis of a wavy joint with T700/SE84HT adherends and Hysol 9430 adhesive. Values up to 19 MPa are obtained in the FE analysis.

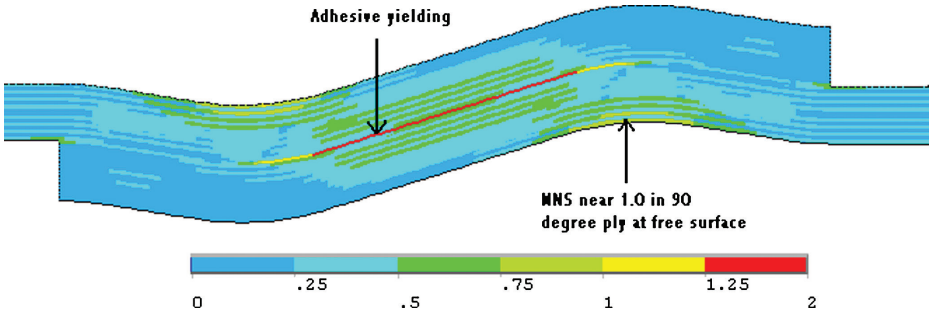

Fig. 10 Contour plot of the parameter MNS obtained from a geometrically nonlinear analysis of a wavy joint with AS4/3501-6 adherends with a $(90,0,90,0)_{2s}$ layup and FM73M film adhesive. Maximum values occur in the adhesive layer and the 90-deg ply closest to the free surface.

analyses were performed: geometrically and materially linear, and geometrically and materially nonlinear. In the latter case the adhesive was modeled as an elastic-plastic material with linear isotropic hardening, whereas the composite was assumed to remain linearly elastic. After yielding, the adhesive was assumed to have a Young's modulus that was 1% of its linear elastic Young's modulus. The results from the different analyses were compared. During geometrically linear cases, the adhesive was also treated as a linear material.

For the wavy joints the end displacements differed very little between the linear and the nonlinear analyses. The difference was more pronounced for the conventional single lap joints. This was also expected and is attributed to the more eccentric design of the conventional single lap joint. The stress fields in the wavy joints obtained from the two analyses (linear and nonlinear) were almost identical. Zeng and Sun[3] drew the same conclusion.

A maximum stress criterion was used to investigate the failure of the T700/SE84HT composite adherends. The tensile and compressive strengths along and perpendicular to the fiber direction as well as the shear strength are listed in Table 6. Failure of the composite

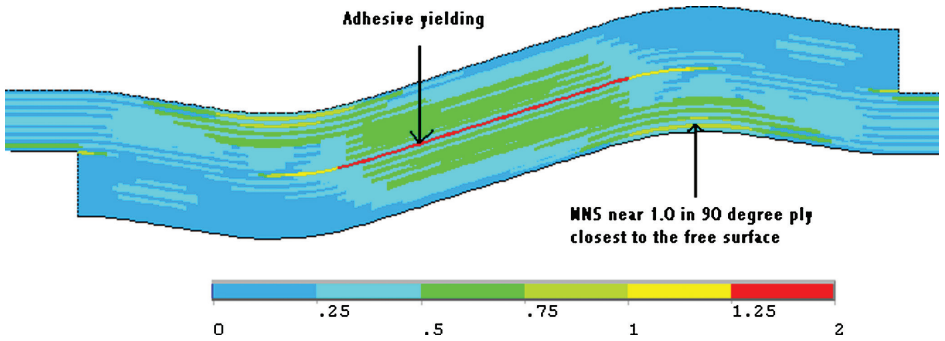

Fig. 11 Contour plot of the parameter MNS obtained from a geometrically nonlinear analysis of a wavy joint with AS4/3501-6 adherends with a $(0,90,0,90)_{2s}$ layup and FM73M film adhesive. Maximum values occur in the adhesive layer and the 90-deg ply closest to the free surface.

material is indicated by a maximum normalized stress (MNS) parameter defined as $\text{MNS} = \max(\sigma_{11}/F_1, \sigma_{22}/F_2, \sigma_{33}/F_2, |\sigma_{12}|/F_6, |\sigma_{13}|/F_6,)$, where the stresses are measured in a local Cartesian coordinate system with the x_1 axis aligned with the fibers and the x_2 axis through the thickness of the ply. (This criterion is not compatible with the transverse isotropy assumed, a fact that was tacitly ignored.) If $\sigma_{11} > 0$, then $F_1 = F_{1t}$; otherwise, $F_1 = F_{1c}$. Similarly, if $\sigma_{22} > 0$ then $F_2 = F_{2t}$; otherwise, $F_2 = F_{2c}$, etc. Failure of the composite would be expected when MNS > 1.0. Figure 7 is a contour plot of the parameter MNS, obtained from a geometrically nonlinear analysis of the conventional single lap joint with an overlap length of 25.4 mm. The highest stresses naturally occur near the ends of the adherends. Some of the stresses are artificial and caused by the sharp reentrant corners and associated singularities that existed in the finite element model, but were not present in the real specimens because of the adhesive making a small fillet at the ends of the adherends. However, it is well known that these regions are most critical, and even simple shear lag models clearly indicate that. It is difficult to estimate the strength of the specimens based on the FE analysis without better knowledge of the behavior of the composite and adhesive when subjected to highly localized loads. Fracture toughness of the composite can play a very important role.

Figure 8 shows a plot of the MNS parameter for the wavy joint, obtained from the nonlinear analysis. As seen in the figure, the highest stresses do not occur near the ends of the adherends, save for possible singular stresses in the reentrant corners. Peak transverse stresses, σ_{22} in a curvilinear Cartesian coordinate system with the x_1 axis aligned with the fibers, are observed to have values between 15 and 20 MPa as seen by the contour plot in Fig. 9. These values are close to the transverse tensile strength of the T700/SE84HT carbon-fiber/epoxy composite as measured in the preceding section. Tensile stress σ_{11} in 90-deg plies (Fig. 8) did reach values above the tensile strengths (MNS > 1.0) as measured in the preceding section, but this would only be expected to lead to transverse matrix cracks and no further damage. Possibly, there would not even be any transverse cracks due to the constraining effect of the adjacent 0-deg plies. MNS also reaches values above 1.0 in the adhesive layer, where yielding occurs. Based on these numerical results and the experiments, the authors' conjecture is that the wavy specimens failed as a result of high transverse tensile stresses in the composite rather than high interfacial stresses. The high transverse tensile strength of the AS4/3501-6 composite (57 MPa) used in Zeng and Sun's specimens allows the benefits of the wavy interfacial stress state to lead to stronger wavy joints.

Joints with the layup used by Zeng and Sun were also analyzed. Linear and nonlinear analyses were performed, employing the same procedure as used earlier. Figure 10 is a contour plot of the parameter MNS, obtained from a geometrically nonlinear analysis of Zeng and Sun's wavy joint with the layup $(90,0,90,0)_{2s}$. Figure 11 displays a similar contour plot for the $(0,90,0,90)_{2s}$ layup. Figures 10 and 11 both show high values of MNS in the adhesive layer where yielding occurs. There appears to be a disparity between the results of the stress analysis performed by Zeng and Sun and that presently performed. The present analysis suggests that Zeng and Sun's $(0,90,0,90)_{2s}$ specimens reached a critical tensile stress (σ_{11})

Table 9 Zeng and Sun's[3] strength data

Layup/geometry	Average P_{cr}, kN	F_x^E, N/mm
$(90,0,90,0)_{2s}$ single lap	4.04	159.06
$(90,0,90,0)_{2s}$ wavy lap	8.65	340.55
$(0,90,0,90)_{2s}$ single lap	6.34	249.61
$(0,90,0,90)_{2s}$ wavy lap	9.86	388.19

in the direction of the specimen in the 90-deg ply closest to the free surface (Fig. 11), whereas shear and transverse tensile stresses remained noncritical. The critical stresses would be expected to lead to transverse matrix cracks, but not to final failure unless the matrix cracks would continue to propagate as interlaminar cracks or delaminations. This might have occurred if the toughness of the interface were low. Zeng and Sun, on the other hand, suggested that the adherends failed in the middle, where two 90-deg plies are adjacent to each other, whereas the present analysis suggests that the stresses there are noncritical (Fig. 11). The strengths used for the AS4/3501-6 carbon/epoxy were 71 MPa in shear and 57 MPa in transverse tension.[3,7]

VI. Comparison with the Zeng and Sun Experiments

Zeng and Sun's[3] tests revealed stronger wavy lap joints in comparison to the conventional single lap joints with the same overlap length of 25.4 mm. Their test results (Table 9) for the $(90,0,90,0)_{2s}$ layup show an average strength of 159.06 and 340.55 N/mm for the conventional single lap and wavy joints, respectively. The $(0,90,0,90)_{2s}$ layup led to average strengths of 249.61 and 388.19 N/mm for the conventional single lap and wavy joints, respectively.

Similar experiments using the T700/SE84HT carbon-fiber/epoxy with a $(0,90,0)_s$ layup and the Hysol 9430 adhesive generally exhibited stronger joints, regardless of the geometry. For overlap lengths of approximately 25.4 mm, the present test results show an average strength of 616.66 and 389.24 N/mm for the conventional single lap and wavy joints, respectively. With this material, however, the conventional single lap configuration was substantially stronger than the wavy configuration proposed by Zeng and Sun.

VII. Conclusions

Experiments performed by Zeng and Sun[3] using AS4/3501-6 carbon epoxy adherends with $(90,0,90,0)_{2s}$ and $(0,90,0,90)_{2s}$ layups, and FM73M film adhesive showed that wavy joints were considerably stronger than conventional single lap joints made with the same materials. This fact was attributed to the interfacial stress profile in the wavy joints in which normal stresses were compressive at the ends and relatively lower in the central region. The experiments associated with this paper using T700/SE84HT carbon epoxy adherends with $(0,90,0)_s$ layup, and Hysol 9430 adhesive showed that wavy joints as proposed by Zeng and Sun were considerably weaker than conventional single lap joints. The present specimens were stronger than those of Zeng and Sun for both geometries. Failure in these

wavy joints was mainly associated with transverse tensile strength. Daniel and Ishai[7] report a transverse tensile strength of 57 MPa for unidirectional AS4/3501-6 carbon epoxy. Experimental testing of the T700/SE84HT $(0,90,0)_s$ layup carbon fiber/epoxy composite revealed a transverse tensile strength of approximately 21 MPa. Finite element analyses suggest that failure occurs because of transverse stress in the wavy joints using the present material. The transverse stresses in the conventional joints were lower for the same applied force (tacitly neglecting the singular stresses in the reentrant corners), thus resulting in a stronger joint. This difference explains the weak performance of the wavy joints in this paper when compared to single lap joints of the same adherends and adhesive. However, the failure strengths of all joints in the present investigation were higher than those measured by Zeng and Sun.

The conventional joints in the present investigation were more than twice as strong as those of Zeng and Sun, and this is believed to be caused by the much higher interlaminar fracture toughness of the present material. The present authors' conjecture is that Zeng and Sun's wavy specimens were stronger than their conventional ones because of reduced stress intensities near the ends of the adherends, and failure in their specimens always initiated there. With the present tougher material failure was not initiated near the ends of the adherends, but rather initiated by high transverse tensile stress in regions far removed from the ends. The fact that the wavy specimens have higher transverse tensile stresses than the conventional ones lead to lower strength of the wavy specimens for the materials used in the present study.

Acknowledgments

This work was supported in part by Pennsylvania Infrastructure Technology Alliance (PITA) Grants PIT-184-99 and PIT-190-00, in part by Office of Naval Research Grant N00014-01-1-0956, and in part by the Department of Mechanical Engineering and Mechanics, Lehigh University. C. T. Sun is acknowledged for kindly sharing his results before publication.

References

[1]Hart-Smith, L. J., "Joints," *Engineered Materials Handbook*, Vol. 1, edited by C. A. Dostal and M. S. Woods, American Society for Materials International, Metals Park, OH, 1987, pp. 479–495.

[2]Hildebrand, M., "The Strength of Adhesive-Bonded Joints Between Fibre-Reinforced Plastics and Metals—Analysis, Shape Optimization and Experiments," VTT Technical Research Centre of Finland, VTT Publications 192, Espoo, Finland, 1994.

[3]Zeng, Q.-G., and Sun, C. T., "Novel Design of a Bonded Lab Joint," *AIAA Journal*, Vol. 39, No. 10, 2001, pp. 1991–1996.

[4]*Annual Book of ASTM Standards*, Vol. 15, American Society for Testing and Materials, West Conshohocken, PA, 2001.

[5]Welsh, J. S., and Adams, D. F., "Unidirectional Composite Compression Strengths Obtained by Testing Cross-Ply Laminates," *Journal of Composites Technology and Research*, Vol. 18, No. 4, 1996, pp. 241–248.

[6]ANSYS, Ver. 5.7.1, Canonsburg, PA, 2001.

[7]Daniel, I. M., and Ishai, O., *Engineering Mechanics of Composite Materials*, Oxford Univ. Press, Oxford, 1994.

E. R. Johnson
Associate Editor